

# The Vortex Core Excitation Spectrum in Gapped Topological d-wave Superconductors

Baruch Rosenstein · Irina Shapiro ·  
Boris Y. Shapiro

Received: 14 June 2013 / Accepted: 28 August 2013 / Published online: 1 October 2013  
© Springer Science+Business Media New York 2013

**Abstract** There are indications that some high temperature unconventional superconductors have a “complex” d-wave order parameter (with an admixture of s-wave) leading to nonzero energy gap. Since the coherence length is short and the Fermi energy is relatively small the quasiclassical approach is inapplicable and the more complicated Bogoliubov-deGennes equations should be used to investigate the excitation spectrum of such a material in a magnetic field. It turns out that equations for the chiral d-wave superconductor simplify considerably and is the basis for any superconductor of that type with a sufficiently large gap. The spectrum of core excitations of the Abrikosov vortex in an anisotropic 3D sample exhibits several features. Unlike in conventional and gapless superconductors the core has a single excitation mode of order energetic gap for each value of momentum along the field. This has a large impact on thermal transport and vortex dynamics.

**Keywords** Chiral d-wave superconductor · Vortex core excitations · Heat transport

## 1 Introduction

Search for new materials exhibiting unconventional superconductivity, initiated by the discovery of the high  $T_c$  cuprates, has become one of the major directions in condensed matter physics. The symmetry of the order parameter is tightly related to

---

B. Rosenstein  
Department of Electrophysics, National Chiao Tung University, Hsinchu, Taiwan, ROC

B. Rosenstein  
Physics Department, Ariel University of Samaria, Ariel 40700, Israel

I. Shapiro · B.Y. Shapiro (✉)  
Department of Physics, Institute of Superconductivity, Bar-Ilan University, Ramat-Gan 52900, Israel  
e-mail: [shapib51@hotmail.com](mailto:shapib51@hotmail.com)

the symmetry of the atomic crystal and the pairing mechanism. The bulk condensate is described by a generally tensorial *complex* order parameter  $\Delta(k)$  exhibiting a great variety of the broken symmetry ground states. A time reversal invariant non s-wave pairing results in nodes in  $k$  space, namely the superconductivity is gapless and the complex nature of the order parameter does not come into play. However when the time reversal is broken, the excitation spectrum becomes gapped. In this case two real nodal pairings  $\Delta_1(k)$  and  $\Delta_2(k)$  form an essentially complex nonvanishing order parameter [1–5],  $\Delta = \Delta_1 + i\Delta_2$  since the nodes of  $\Delta_1$  and  $\Delta_2$  appear typically along non intersecting lines in momentum space.

The first system exhibiting the gap originating this way was liquid He<sup>3</sup>. In its ABM phase even the extreme case of that phenomenon, the so-called chiral superconductivity [6, 7], characterized by presence of electron-hole symmetry and absence of both the time-reversal and spin-rotation symmetry, appears. In this case  $\Delta_1 = p_x$  and  $\Delta_2 = p_y$  are combined into  $\Delta = p_x + ip_y$  with “equal strength”. Charged spin-triplet superfluids, like [8, 9] Sr<sub>2</sub>RuO<sub>4</sub> and heavy fermion UPt<sub>3</sub> were shown to have similar structure, although it is not yet clear whether they are chiral. A recently discovered Cu-doped topological superconductor Bi<sub>2</sub>Se<sub>3</sub> produces an equivalent chiral pseudospin system on its surface [10, 11]. The surface states in these materials attract much attention these days because they are recognized as Majorana fermion bound states [12–17].

Despite a widely held opinion that most high  $T_c$  cuprates have nodes and thus are gapless (originating from seminal experiments Tsuei and Kirtley [18]), there have always existed a descent opinion [19]. Very recently the fully gapped state was clearly demonstrated in nano-sized YBa<sub>2</sub>Cu<sub>3</sub>O<sub>7</sub> islands [20, 21]. Charging of the YBCO grains allows an extremely precise determination of the energy required to add single electron to the grain. This is consistent with earlier STM evidence [22] of significant admixture of  $id_{xy}$  in Ca doped YBCO. The minority pairing was theoretically supported [23] by a microscopic model of hybridization between  $d_{x^2-y^2}$  and  $d_{xy}$ . In particular topologically nontrivial superconducting state of two-dimensional electron system with large center-of-mass pair momentum under predominant repulsive screened Coulomb interaction was considered. Direct numerical solution of the self-consistency equation exhibits two nearly degenerate order parameters  $d_{x^2-y^2}$  and  $d_{xy}$ . Spontaneous breaking of the time-reversal symmetry can mix these states and even form chiral  $d + id$  superconducting states.

On general ground it was argued [6, 7] that the atomic lattice can act as a custodial symmetry to ensure degeneracy of different superconducting instabilities. In such a case the degeneracy is linked to higher dimensional irreducible representations of the lattice symmetry group, and a chiral superposition of superconducting states can be energetically favorable below  $T_c$ . Cuprates (with an exception of YBCO) are four-fold symmetric. It was pointed out recently [24] that for the square lattice and its  $C_{4v}$  group, there is no representation for singlet Cooper pairs that could result in chiral superconductivity. This, however, changes for hexagonal systems, where the  $E_2$  representation of the  $C_{6v}$  lattice symmetry group implies the degeneracy of the  $d_{x^2-y^2}$  and  $d_{xy}$  wave state at the instability level which can yield a chiral  $d + id$  singlet superconductor. Degeneration of the  $d_{x^2-y^2}$  and  $d_{xy}$  ordered states inherent in doped graphene monolayer has been recently considered by Nandkishore et al. [25] as a

possible origin of a rise of a singlet chiral superconducting (SC) state with  $d + id$  orbital symmetry. In addition there exists a theoretical expectation of superconductivity in doped graphene creating a chiral d-wave superconductivity, see [5, 26–29]. In addition chiral d-wave superconductivity (Chern number  $\pm 2$ ) has been proposed for  $\text{Na}_x\text{CoO}_2 \cdot y\text{H}_2\text{O}_{12-15}$ , a novel heavy fermionic compound [30, 31]. Note that all these systems have small Fermi momentum  $k_F$  of the order of magnitude of the inverse coherence length  $\xi^{-1}$ .

Magnetic fields in type II superconducting film easily create stable line-like topological defects, Abrikosov vortices [32, 33]. In the simplest vortex the phase of the order parameter rotates by  $2\pi$  around the vortex and each vortex carries a unit of magnetic flux  $\Phi_0$ . Quasiparticles near the vortex core “feel” the phase wind by creating a set of discrete low-energy Andreev bound states. For the s-wave superconductors when the vortices are unpinned (freely moving) these states were comprehensively studied theoretically including the excitations spectrum [34, 35], density of states [36–39], their role in vortex viscosity [32, 33], and the microwave absorption [40]. The low lying spectra of quasiparticles and hole excitations are equidistant,  $E_l = l\Delta^2/E_F$ , where the angular momentum  $l$  takes on half integer values. The “minigap” in the low  $T_c$  s-wave superfluids is of order of  $\Delta^2/E_F$ . Since the Fermi energy  $E_F \gg \Delta$  it is equivalent in the clean limit to large values of dimensionless parameter  $k_F\xi \gg 1$ . Roughly there are Andreev bound states below the superconducting threshold.

Free vortices in the chiral p-wave superconductors exhibit a remarkable topological feature of appearance of the zero energy mode in the vortex core [41]. The spectrum of the low energy excitations remains equidistant,  $E_l = (l - 1)\Delta^2/E_F$ , but now  $l$  is integer [1–4]. The zero mode represents a condensed matter analog of the Majorana fermion first noticed in elementary particle physics [42]. While the minigap in the s and d-wave superconductors was detected by STM, in p-wave has not yet been observed. The major reason for that is the *small value of the minigap* in the core spectrum (just mK for  $\text{Sr}_2\text{RuO}_4$ ). It was shown theoretically [43, 44] that in the s-wave superconductors pinning by an inclusion of radius of just  $R = 0.2\xi - 0.5\xi$  changes dramatically the subgap excitation spectrum: the minigap  $\Delta^2/E_F$  becomes of the order of  $\Delta$ . On the other hand in the chiral p-wave superconductors the spectrum of the core excitations of the charged states for  $R = 0.1\xi - 0.4\xi$  is less sensitive to the inclusion, but nevertheless pushes the spectrum up towards  $\Delta$ , so that they therefore interfere less with the Majorana state that is topologically protected and cannot be affected by the inclusion [45].

In a magnetic field the nodal  $d_{x^2-y^2}$  superconductor the spectrum of Andreev states of single vortex was calculated by Kopnin [46] under assumption of  $\gamma^{-1} = 2k_F\xi \gg 1$ . The condition allows the use of semiclassical approximation. He found the spectrum to be similar to that of the s-wave superconductor despite the nodes. Maki [47] extended the work beyond the semiclassical approximation and found that there is a series of additional extended states along the node directions. The low-energy states have no counterpart in a vortex of s-wave superconductors. While in conventional superconductors,  $k_F\xi \gg 1$  in “bad metals”, where the coherence length only slightly exceeds the inter-electron distance  $k_F^{-1}$ , resulting in  $k_F\xi \geq 1$ . Analyzing the STM experiments, Maki and coworkers [48, 49] found that in high  $T_c$  cuprate

YBCO the parameter  $\gamma$  is of order 1. This modifies significantly the spectrum. It contains just a few Andreev states in addition to the node extended states. The situation is expected to be different in d-wave gapped superconductors with  $\gamma^{-1} \sim 1$  discussed above and therefore the nodal states should disappear. The number of Andreev states should be small and could not be treated semiclassically. He pointed out that the system of Bogoliubov-deGennes equations for d-wave superconductors does not separate into a set of equations for each angular momentum  $l$  unlike that of the s-wave and chiral p-wave. Therefore beyond the semiclassical approximation all the angular momenta mix and one is forced [48, 49] to truncate the series.

We found that the situation is different for chiral d-wave case: the system does separate into groups of two harmonics making its solution possible. For a gapped non-chiral superconductor one can develop the perturbation theory around the chiral limit. We perform this calculation for  $\gamma \sim 1$  and extend the work to 3D anisotropic superconductors not considered in [48, 49]. We compute the density of states and thermal conductivity along the field direction (the vortex axis) that can be effectively used along with STM [50–52] and microwave radiation to detect the features of the pairing.

## 2 The BdG Equations for General d-wave Superconductor

### 2.1 Microscopic Definition of the Gap Operator

We begin with the nonlocal BdG equations for the Bogoliubov eigenfunction corresponding to the eigen energy  $E_n$ ,

$$\begin{pmatrix} \hat{H}_0 & \hat{\Delta} \\ \hat{\Delta}^+ & -\hat{H}_0^* \end{pmatrix} \begin{pmatrix} u_n \\ v_n \end{pmatrix} = E_n \begin{pmatrix} u_n \\ v_n \end{pmatrix}. \quad (1)$$

As a single particle Hamiltonian one can take the parabolic dispersion and the approximation

$$H_0 = \frac{1}{2m} \left( \mathbf{p} - \frac{e}{c} \mathbf{A} \right)^2 - E_F, \quad (2)$$

where  $E_F$  is the Fermi energy. The gap function in an unconventional superconductor [53] is characterized by the nonlocal “order parameter” operator,

$$\hat{\Delta}g = \int \Delta(\mathbf{r}, \mathbf{r}') g(\mathbf{r}') d\mathbf{r}'. \quad (3)$$

Within the BCS theory the kernel  $\Delta(r, r')$  is subject to the self-consistency condition:

$$\Delta(\mathbf{r}, \mathbf{r}') = \frac{V(\mathbf{r} - \mathbf{r}')}{2} \sum_n [u_n(\mathbf{r}) v_n^*(\mathbf{r}') + u_n(\mathbf{r}') v_n^*(\mathbf{r})] \tanh\left(-\frac{E_n}{2T}\right), \quad (4)$$

where  $V(r - r')$  is the pairing interaction and  $k_B$  will be set to 1.

The vector potential  $\mathbf{A}$  for a single vortex has, in polar coordinates,  $r, \varphi$ , only an azimuthal component  $A_\varphi(r)$  and in the London gauge consists of the singular part  $A_\varphi^s = hc/2er$  (field of the infinitely thin solenoid) and typically a rather insignificant regular part that does not carry flux. Neglecting the regular part [1–4], the singular one can be “compensated” by the transformation [54]:

$$\begin{pmatrix} u_n \\ v_n \end{pmatrix} \rightarrow \begin{pmatrix} u_n e^{-i\varphi/2} \\ v_n e^{i\varphi/2} \end{pmatrix}, \quad \Delta(\mathbf{r}, \mathbf{r}') \rightarrow \Delta(\mathbf{r}, \mathbf{r}') e^{-i\varphi}. \tag{5}$$

After this transformation the Hamiltonian  $H_0$  has the form

$$H_0 = -\frac{\hbar^2}{2m_\perp} \nabla_\perp^2 - \frac{\hbar^2}{2m_z} \partial_z^2 - E_F. \tag{6}$$

Introducing the center-of-mass coordinate,  $\mathbf{R} = (\mathbf{r} + \mathbf{r}')/2, \mathbf{s} = \mathbf{r} - \mathbf{r}'$  one makes a partial Fourier representation

$$\Delta(\mathbf{R}, \mathbf{s}) = \frac{1}{(2\pi)^2} \int d\mathbf{k} \Delta(\mathbf{R}, \mathbf{k}) e^{i\mathbf{k}\cdot\mathbf{s}}. \tag{7}$$

Expanding  $\Delta(\mathbf{R}, \mathbf{k})$  to second order in  $\mathbf{k}$ ,

$$\Delta(\mathbf{R}, \mathbf{k}) = \Delta_{x^2-y^2}(R)(k_x^2 - k_y^2) + i \Delta_{xy}(R)k_x k_y, \tag{8}$$

and substituting it into Eq. (7), one obtains, after integration by parts, a local form [55, 56] of the order parameter operator:

$$\widehat{\Delta} = -\frac{\Delta_0}{4k_F^2} (\widehat{L}_{xx} - \widehat{L}_{yy} + 2i\alpha \widehat{L}_{xy}). \tag{9}$$

Here the same operators are written via derivatives on the mesoscopic scale:

$$\widehat{L}_{ij} \equiv \{\partial_i, \{\partial_j, \Theta(R)e^{-i\varphi}\}\}, \tag{10}$$

for  $i = x, y$ , while anti-commutator was defined as  $\{\widehat{a}, \widehat{b}\} \equiv \widehat{a}\widehat{b} + \widehat{b}\widehat{a}$ .

Thus the spatial part of the order parameter  $\Delta_{x^2-y^2}(R) = \Delta_0 \Theta(R)$  is normalized by the “isotropic” gap parameter  $\Delta_0$ . We assume for simplicity that the spatial dependence of the two components is the same  $\Delta_{xy}(R) = \alpha \Delta_0 \Theta(R)$ . We also assume that both components of the order parameters vanish at the same point, otherwise the problem becomes much more complicated and more general Ansatz should be used [57, 58]. (It is not obvious that the vortex centers in different order parameter components should coincide. In principal the interaction of the components might be responsible for the formation of non-singular vortices. This case should be considered separately.)

## 2.2 The Chiral Representation of the Order Parameter

Let us introduce the following “chiral” operators,

$$L_{++} = \{\partial_+, X_+\} = L_{xx} - L_{yy} + 2iL_{xy}, \tag{11}$$

$$L_{--} = \{\partial_-, Y_-\} = L_{xx} - L_{yy} - 2iL_{xy}, \quad (12)$$

$$L_{+-} = L_{xx} + L_{yy} + iL_{xy}, \quad (13)$$

where  $\partial_{\pm} = \partial_x \pm i\partial_y$ , and

$$X_{\pm} = \{\partial_{\pm}, \Theta e^{\mp i\varphi}\}; \quad Y_{\pm} = \{\partial_{\pm}, \Theta e^{\pm i\varphi}\}. \quad (14)$$

In terms of these operators one can write

$$L_{xx} = \frac{1}{4}(L_{++} + L_{--} + 2L_{+-}), \quad (15)$$

$$L_{yy} = \frac{1}{4}(-L_{++} - L_{--} + 2L_{+-}), \quad (16)$$

$$L_{xx} - L_{yy} = \frac{1}{2}(L_{++} + L_{--}); \quad L_{xy} = -\frac{i}{4}(L_{++} - L_{--}). \quad (17)$$

Substituting Eqs. (15, 16) and Eq. (17) into Eqs. (6, 9), one obtains in this representation:

$$H_0 = -\frac{\hbar^2}{2m_{\perp}}L_+L_- - \frac{\hbar^2}{2m_z}\partial_z^2 - E_F; \quad (18)$$

$$\widehat{\Delta} = -\frac{\Delta_0}{8k_F^2}(L_{++}(1 + \alpha) + L_{--}(1 - \alpha)). \quad (19)$$

### 2.3 Polar Coordinates

In polar coordinates,

$$\partial_x = -\frac{1}{r}\sin\varphi\partial_{\varphi} + \cos\varphi\partial_r; \quad (20)$$

$$\partial_y = \frac{1}{r}\cos\varphi\partial_{\varphi} + \sin\varphi\partial_r, \quad (21)$$

the chiral combinations are

$$\partial_{\pm} = e^{\pm i\varphi}\left(\partial_r \pm \frac{i}{r}\partial_{\varphi}\right). \quad (22)$$

The diagonal part of the BdG Hamiltonian takes the form

$$H_0 = -\frac{\hbar^2}{2m_{\perp}}\left(\frac{1}{r}\partial_r + \partial_r^2 + \frac{1}{r^2}\partial_{\varphi}^2\right) - \frac{\hbar^2}{2m_z}\partial_z^2 - E_F. \quad (23)$$

The off diagonal terms in Eqs. (5) include:

$$\begin{aligned} L_{++}e^{i\varphi/2}v_n &= e^{3i\varphi/2}Mv_n; \quad L_{++}^+e^{-i\varphi/2}u_n = e^{-3i\varphi/2}M^+u_n; \\ L_{--}e^{i\varphi/2}v_n &= e^{-i\varphi/2}Nv_n; \quad L_{--}^+e^{-i\varphi/2} = e^{i\varphi/2}N^+v_n, \end{aligned} \quad (24)$$

where

$$M = \Theta'' - \frac{\Theta'}{r} + \frac{2\Theta}{r^2} + 4\Theta'\partial_r - \frac{4\Theta}{r}\partial_r + \frac{4i}{r}\Theta'\partial_\varphi - \frac{8i\Theta}{r^2}\partial_\varphi + 4\Theta\partial_r^2 + \frac{8i\Theta}{r}\partial_r\partial_\varphi - \frac{4\Theta}{r^2}\partial_\varphi^2; \tag{25}$$

$$N = \Theta'' + \frac{3\Theta'}{r} - \frac{2\Theta}{r^2} + 4\Theta'\partial_r + \frac{4\Theta}{r}\partial_r - 4i\frac{\Theta'}{r}\partial_\varphi - \frac{2i\Theta}{r^2}\partial_\varphi + 4\Theta\partial_r^2 - 8i\frac{\Theta}{r}\partial_r\partial_\varphi - \frac{4\Theta}{r^2}\partial_\varphi^2. \tag{26}$$

### 3 Solution of the BDG Equations

#### 3.1 Decoupling of Different Angular Momenta in Chiral Superconductor

Let us consider the chiral case of  $\alpha = 1$  in Eq. (9). The set of BdG equation in this case is

$$\begin{pmatrix} \hat{H}_0 & -\frac{\Delta_0}{k_F^2}e^{2i\varphi}\hat{M} \\ -\frac{\Delta_0}{k_F^2}e^{-2i\varphi}\hat{M}^+ & -\hat{H}_0^* \end{pmatrix} \begin{pmatrix} u_n \\ v_n \end{pmatrix} = E_n \begin{pmatrix} u_n \\ v_n \end{pmatrix}. \tag{27}$$

Using the translation symmetry in the field direction, the operator  $H_0$  for component with momentum  $k_z$  takes the form

$$\hat{H}_0 = -\frac{\hbar^2}{2m_\perp} \left( \frac{1}{r}\partial_r + \partial_r^2 + \frac{1}{r^2}\partial_\varphi^2 \right) - E_\perp, \tag{28}$$

where  $E_\perp = E_F - k_z^2/2m_z$ . Despite the fact that there is no explicit rotational symmetry, it is convenient to use the 2D angular momentum basis

$$\begin{pmatrix} u \\ v \end{pmatrix} = \sum_l e^{il\varphi} \begin{pmatrix} u_l(r) \\ v_l(r) \end{pmatrix}; \tag{29}$$

which leads to

$$Eu_l = e^{-il\varphi}\hat{H}_0e^{il\varphi}u_l - \frac{\Delta_0}{4k_F^2}e^{i(2-l)\varphi}\hat{M}e^{i(l-2)\varphi}v_{l-2} \tag{30}$$

$$Ev_l = -e^{-il\varphi}\hat{H}_0e^{il\varphi}v_l - \frac{\Delta_0}{4k_F^2}e^{-i(l+2)\varphi}\hat{M}^+e^{i(l+2)\varphi}u_{l+2}.$$

With the transition to energies in units of  $\Delta_0$ , in particular  $\varepsilon_n = E_n/\Delta_0$  and distances in units of coherence length ( $\xi = \hbar v_F/\Delta_0$  in the clean limit),  $r \rightarrow r/\xi$ ,  $k_z \rightarrow \xi k_z$ ,  $k_\perp \rightarrow \xi k_\perp$ , the equations become:

$$\varepsilon u_l = -\gamma \left( \partial_r^2 + \frac{1}{r}\partial_r + k_\perp^2 - \frac{l^2}{r^2} \right) u_l - \gamma^2 \Pi_l v_{l-2}; \tag{31}$$

$$\begin{aligned} \Pi_1 = & \left( \Theta'' + \frac{4l-9}{r} \Theta' + 2 \frac{2l^2 - 12l + 17}{r^2} \Theta + 4\Theta' \partial_r \right. \\ & \left. + 4 \frac{2l-5}{r} \Theta \partial_r + 4\Theta \partial_r^2 \right), \end{aligned} \quad (32)$$

$$\varepsilon v_l = -\gamma^2 \Pi_2 u_{l+2} + \gamma \left( \partial_r^2 + \frac{1}{r} \partial_r + k_\perp^2 - \frac{l^2}{r^2} \right) v_l,$$

$$\begin{aligned} \Pi_2 = & \left( \Theta'' - \frac{4l+9}{r} \Theta' + 2 \frac{2l^2 + 12l + 17}{r^2} \Theta + 4\Theta' \partial_r - 4 \frac{2l+5}{r} \Theta \partial_r \right. \\ & \left. + 4\Theta \partial_r^2 \right), \end{aligned} \quad (33)$$

where only two dimensionless parameters enter. One is  $k_\perp \xi$  and the second is

$$\gamma = \frac{\Delta_0}{4E_F} = \frac{1}{2k_F \xi}. \quad (34)$$

One observes that the equations decouple if one chooses in the second equation angular momentum  $l-2$ :

$$\varepsilon u_l = -\gamma \left( \partial_r^2 + \frac{1}{r} \partial_r + k_\perp^2 - \frac{l^2}{r^2} \right) u_l - \gamma^2 \Pi_3 v_{l-2}; \quad (35)$$

$$\begin{aligned} \Pi_3 = & \left( \Theta'' + \frac{4l-9}{r} \Theta' + 2 \frac{2l^2 - 12l + 17}{r^2} \Theta + 4\Theta' \partial_r \right. \\ & \left. + 4 \frac{2l-5}{r} \Theta \partial_r + 4\Theta \partial_r^2 \right), \end{aligned} \quad (36)$$

$$\varepsilon v_{l-2} = -\gamma^2 \Pi_4 u_l + \gamma \left( \partial_r^2 + \frac{1}{r} \partial_r + k_\perp^2 - \frac{(l-2)^2}{r^2} \right) v_{l-2},$$

$$\begin{aligned} \Pi_4 = & \left( \Theta'' - \frac{4l+1}{r} \Theta' + 2 \frac{2l^2 + 4l + 1}{r^2} \Theta + 4\Theta' \partial_r - 4 \frac{2l+1}{r} \Theta \partial_r \right. \\ & \left. + 4\Theta \partial_r^2 \right). \end{aligned} \quad (37)$$

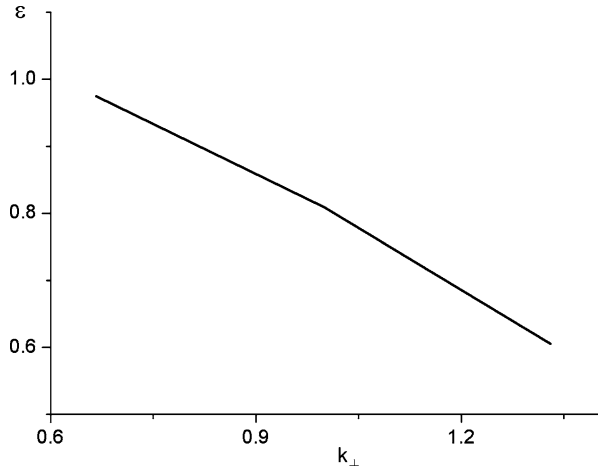
The profile of the order parameter  $\Theta(r)$  should be calculated self consistently, however we used a simple dependence  $\Theta(r) = \tanh(r)$ . This is justified a posteriori by the local density of states (LDOS) that shows that it is completely dominated by the continuum states rather than the few Andreev states.

### 3.2 Results for the Spectrum and Charge Density for a Single Vortex

This was solved numerically with boundary conditions  $u_l(r=0) = v_l(r=0) = 0$  and  $u_l(r=L) = v_l(r=L) = 0$ , where  $L$  is the radius of the cylindrical sample (disc



**Fig. 1** A single Andreev state energy as function of  $k_{\perp}$ . The value of the only parameter characterizing the system is  $\gamma = 0.38$ . The dispersion relation is nearly linear up to a threshold at  $\Delta$



when the width of the sample is finite  $-L_z/2 < z < L_z/2$ ). Pinned vortices are discussed in the next section. The Andreev bound state is found for  $\gamma = 0.38$  only for  $l = 1$ . The energy as function of  $k_{\perp}$  for  $\gamma = 0.38$  is presented in Fig. 1. All the other angular momentum channels have just the continuum above the superconducting threshold. Moreover it appears only for

$$k_z < k_z^{\max} = 2/\gamma \tag{38}$$

since  $E_{\perp}$  should be positive. This is a direct consequence of  $\gamma \sim 1$ . For small  $\gamma$  the spectrum of Andreev states is semiclassical as discussed in the Introduction. The “minigap” therefore is very large and it is difficult to excite the core states. The Andreev states (one for each available value of  $k_z$ ) are localized near the core, see the radial density

$$\rho(r) = 2\pi r (|u_1(r)|^2 + |v_1(r)|^2) \tag{39}$$

in Fig. 2. The core states come mostly from the particle rather than the hole sector for the given direction of the magnetic field, so there is a sizable charge density in the hole. The contributions from the continuum above the threshold are expected to compensate each other since they originate both from electron and hole excitations. The density of states reads:

$$\begin{aligned} N(r, \varepsilon) &= \sum_n \{ |u_n(r)|^2 \delta(\varepsilon - \varepsilon_n) + |v_n(r)|^2 \delta(\varepsilon + \varepsilon_n) \} \\ &= \frac{|u_1(r)|^2}{\sqrt{\varepsilon - \varepsilon_1(0)}} + \sum_{cont} \left\{ \frac{|u_n(r)|^2}{\sqrt{\varepsilon - \varepsilon_n(0)}} + \frac{|v_n(r)|^2}{\sqrt{\varepsilon + \varepsilon_n(0)}} \right\}. \end{aligned} \tag{40}$$

### 3.3 Generalization to the Non-chiral Case and to Pinned Vortices

Generally the d-wave order parameter, Eq. (19), deviates from “perfect chirality”,  $\alpha = \pm 1$ , Small deviations from the positive chirality can be parametrized by  $\zeta$ ,

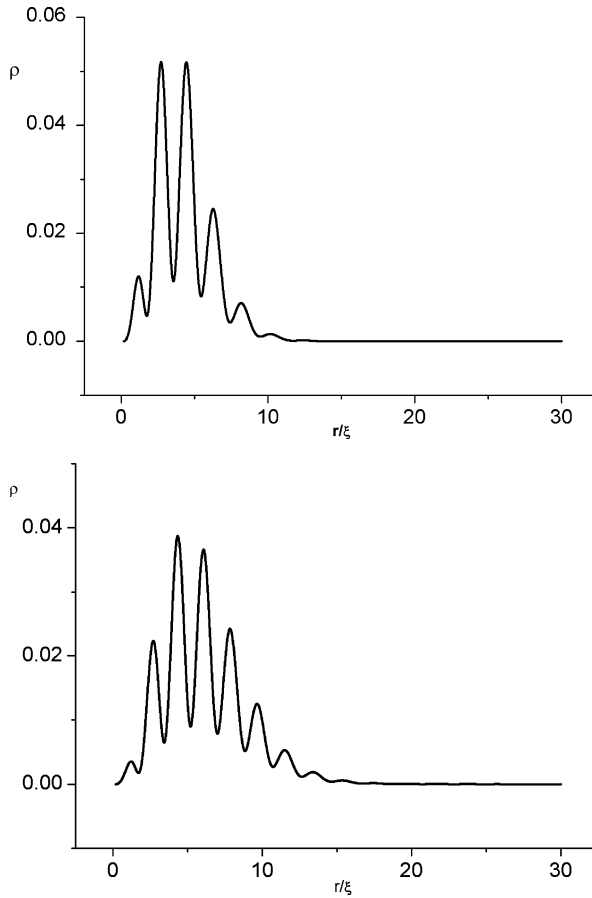


**Fig. 2** The radial density  $\rho(r)$ , Eq. (39), of the core state as function of the distance from the vortex center for  $\gamma = 0.38$ . It extends several coherence lengths inside the superconductor. Two values of the momentum along the magnetic field direction  $k_z$  are given **a**  $k_z = 0.88/\xi$ . **b**  $k_z = 1.15/\xi$

$$\alpha = 1 + 2\zeta:$$

$$\widehat{\Delta} = -\frac{\Delta_0}{4k_F^2}L_{++} - \zeta \frac{\Delta_0}{4k_F^2}(L_{++} - L_{--}). \tag{41}$$

The correction therefore can be written using Eq. (17) as

$$V = -i\zeta \frac{\Delta_0}{k_F^2}L_{xy}. \tag{42}$$

The shift of the Andreev eigenstates energy occurs only in second order in  $\zeta$  since

$$\Delta\varepsilon_1 = -i\zeta \frac{\Delta_0}{k_F^2} \int_{r=0}^L r \int_{\varphi} \langle l=1|L_{++}|l=1\rangle + cc = 0. \tag{43}$$

The Andreev state goes lower therefore only when the energy gap  $\Delta = \Delta_0(1 - 2\zeta)$  is significantly (first order in  $\zeta$ ) smaller than  $\Delta_0$ . We expect that for yet lower  $\alpha$  the spectrum at  $\gamma \sim 1$  will still consist of just one Andreev state in the  $l = 1$  channel.

Till now the boundary condition at the center of the vortex was free. One can describe a pinned vortex by a different boundary condition,  $u_l(r = R) = v_l(r = R) = 0$ , where  $R$  is the radius of the pinning area of order  $\xi$  (assumed for simplicity dielectric). The results do not change appreciably until the radius exceeds  $\xi$ .

## 4 Thermal Transport

### 4.1 Kopnin-Landauer Formula

Thermal conductivity is an effective tool to demonstrate the minigap due to activated behavior of the electron contribution. To calculate the quasiparticle contribution to thermal conductivity along the vortex cores when the upper side of the vortex line is held at temperature  $T_1$  and the lower side at temperature  $T_2$ , we use a general ballistic (width of the film  $L_z$  smaller than the mean free path) Kopnin-Landauer formula [59, 60]. The heat current at temperature lower than the threshold to the continuum of states is carried mainly by the bound core states. For a single vortex in a sufficiently thick sample the variable  $k_z$  can be considered as a continuous one and the thermal current can be written as

$$I(T) = \int_0^{k_z^{\max}} \frac{dk_z}{2\pi\hbar} \left| \frac{dE_1(\gamma, \xi k_z)}{dk_z} \right| \frac{E_1(\gamma, \xi k_z)}{1 + \exp(E_1(\gamma, \xi k_z)/T)} \tag{44}$$

$$= \frac{\Delta_0^2}{2\pi\hbar} \int_0^{k_z^{\max}\xi} d\tilde{k}_z \frac{d\varepsilon_1(\gamma, \tilde{k}_z)}{d\tilde{k}_z} \frac{\varepsilon_1(\gamma, \tilde{k}_z)}{1 + \exp(\varepsilon_1(\gamma, \tilde{k}_z)/t)}, \tag{45}$$

where  $t = T/\Delta_0$  and  $\tilde{k}_z = \xi k_z$ . Changing variables one obtains

$$I(T) = \frac{\Delta_0^2}{2\pi\hbar} \int_1^{2/\gamma} \frac{\varepsilon d\varepsilon}{1 + \exp(\varepsilon/t)} = \frac{T^2}{2\pi\hbar} \left[ \Pi\left(\frac{\Delta_0}{T}\right) - \Pi\left(\frac{8E_F}{T}\right) \right]. \tag{46}$$

Here the lower limit of integration is the energy for  $k_z = 0$  and the indefinite integral is

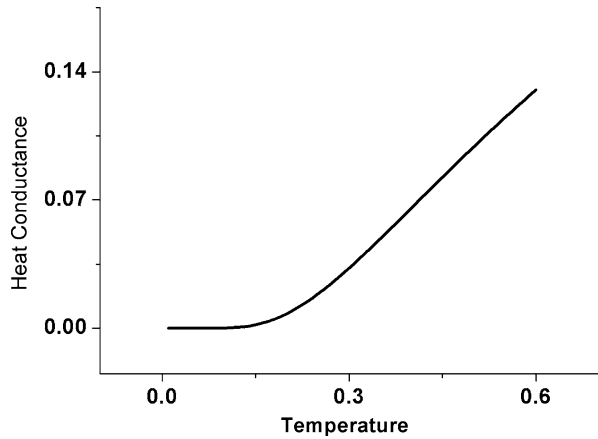
$$\Pi(\varepsilon) = \int \frac{\varepsilon d\varepsilon}{1 + \exp(\varepsilon)} = -\varepsilon^2/2 + \varepsilon \log(1 + e^\varepsilon) + Li_2(-e^\varepsilon), \tag{47}$$

where  $Li$  is the polylog function. For small temperature differences the linear response can be used,

$$\frac{dI}{dT} = \frac{T}{\pi\hbar} \left[ \Pi\left(\frac{\Delta_0}{T}\right) + \frac{\Delta_0^2/2T^2}{1 + \exp(\Delta_0/T)} - \Pi\left(\frac{8E_F}{T}\right) - \frac{32E_F^2/T^2}{1 + \exp(8E_F/T)} \right]. \tag{48}$$

In Fig. 3 the heat conductance of a single vortex line is given as function of the inverse temperature (in units of  $\Delta^{-1}$ ) demonstrating the activated behavior of the electron contribution.

**Fig. 3** Heat flow through a superconductor in a magnetic field along the vortex cores. The temperature difference between the bottom and the top contacts leads to energy flow carried at low temperatures by the core states. Dimensionless heat conductance  $\frac{\hbar}{\Delta} \frac{dI}{dT}$  of a single vortex given in Eq. (48) as function of temperature in units of  $\Delta$



## 5 Conclusion and Discussion

To summarize, in the gapped  $d_{x^2-y^2} + i\alpha d_{xy}$  unconventional (in the sense of  $E_F$  being of the same order of magnitude as  $\Delta$ ) superconductor in a magnetic field the spectrum consists of a single excitation mode for any value of momentum  $k_z$  along the field per Abrikosov vortex. Therefore each vortex core can be viewed as a nanosize normal “quantum wire” inside the superconducting material. The dispersion in this one-dimensional metallic system is roughly linear as a function of  $k_\perp$ , see Fig. 1. Unlike the extended Andreev states found in a better studied theoretically case of the nodal  $d_{x^2-y^2}$  case [47], the core states are well localized, see Fig. 2.

Due to the exceptionally large “minigap” it is difficult to excite the 1D quantum wire mechanically, thermally or electromagnetically. This has a large impact on the thermal transport along the field direction and vortex dynamics in the direction perpendicular to the field. At temperatures lower than  $\Delta/2$  the viscosity should be very large, while the thermal transport has an activated nature see Fig. 3. In particular case the critical current in such superconductors would be greatly enhanced at these temperatures. A magnetic field  $B \gg H_{c1}$  creates  $SB/\Phi_0$  vortices over area  $S$ , so that heat conductivity is  $\kappa = \frac{L_z B}{\Phi_0} \frac{dI}{dT}$ , where  $L_z$  is the sample width. For  $B = 5$  T (between  $H_{c1}$  and  $H_{c2}$  for cuprates), with  $L_z = 70$  nm at  $T/\Delta = 0.2$  one obtains a thermal conductivity of order  $\kappa \sim 10^2$  W/K m.

Technically, since the coherence length is short and the Fermi energy is relatively small, the quasiclassical approach is inapplicable and more complicated Bogoliubov-deGennes equations were used. The approach simplifies for the chiral d-wave superconductor,  $\alpha = \pm 1$ , due to the decoupling of sectors in the BdG equation with different angular momentum  $l$ . Despite the fact that the angular momentum is not a conserved quantum number, it can be used to label Andreev bound states. It turns out that such states exist only in the  $l = 1$  channel. The approach can be generalized for any superconductor of that type with a sufficiently large gap. A natural and rather direct method to look for evidence for chiral d-wave superconductors is microwave absorption by the vortex core states in a magnetic field. In this case the absorption depends strongly on the polarization of the incident wave [61, 62].

Vortices are typically organized in the hexagonal vortex lattice that leads to the creation of a narrow band due to small overlaps of the Andreev states belonging to the neighboring vortex cores. Periodicity however is not expected to play a role in thermal conductivity along the “nano-wires” that are well separated.

**Acknowledgements** B.Y.S. and I.S. acknowledge support from the Israel Scientific Foundation.

## References

1. M. Matsumoto, M. Sigrist, J. Phys. Soc. Jpn. **68**, 724 (1999)
2. C.-K. Lu, S.-K. Yip, Phys. Rev. B **78**, 132502 (2008)
3. S. Fujimoto, Phys. Rev. B **77**, 220501(R) (2008)
4. M. Sato, S. Fujimoto, Phys. Rev. B **79**, 094504 (2009)
5. A.M. Black-Schaffer, Phys. Rev. Lett. **109**, 197001 (2012)
6. A.J. Leggett, Rev. Mod. Phys. **47**, 331 (1975)
7. A.J. Leggett, *Quantum Liquid: Bose Condensation and Cooper Pairing in Condensed-Matter Systems* (Oxford University Press, Oxford, 2006)
8. Y. Maeno, H. Hashimoto, K. Yoshida, S. Nishizaki, T. Fujita, J.G. Bednorz, F. Lichtenberg, Nature **372**, 532 (1994)
9. A.P. Mackenzie, Y. Maeno, Rev. Mod. Phys. **75**, 657 (2003)
10. Y.S. Hor et al., Phys. Rev. Lett. **104**, 057001 (2010)
11. L.A. Wray, Nat. Phys. **6**, 855 (2010)
12. N. Read, D. Green, Phys. Rev. B **61**, 10267 (2000)
13. C.J. Bolech, E. Demler, Phys. Rev. Lett. **98**, 237002 (2007), 43
14. K. Sengupta, I. Zutic, H.-J. Kwon, V.M. Yakovenko, S. Das Sarma, Phys. Rev. B **63**, 144531 (2001)
15. A.Y. Kitaev, Phys. Usp. **44**, 131 (2001)
16. D.A. Ivanov, Phys. Rev. Lett. **86**, 268 (2001)
17. S. Das Sarma, C. Nayak, S. Tewari, Phys. Rev. B **73**, 220502(R) (2006)
18. C.C. Tsui, J.R. Kirtley, Rev. Mod. Phys. **72**, 969 (2000)
19. M. Franz, Z. Tešanović, Phys. Rev. Lett. **80**, 4763 (1998)
20. A.M. Black-Schaffer, D.S. Golubev, T. Bauch, F. Lombardi, M. Fogelström, Phys. Rev. Lett. **110**, 197001 (2013)
21. D. Gustafsson et al., Nat. Nanotechnol. **8**, 25 (2013)
22. J.H. Ngai, R. Beck, G. Leibovitch, G. Deutscher, J.Y.T. Wei, Phys. Rev. B **82**, 054505 (2010)
23. V.I. Belyavsky, V.V. Kapaev, Yu.V. Kopaev, Pis'ma ZhETF **96**, 809 (2012). JETP Lett. **96**, 724 (2013)
24. M.L. Kiesel, C. Platt, W. Hanke, D.A. Abanin, R. Thomale, Phys. Rev. B **86**, 020507 (2012)
25. R. Nandkishore, L.S. Levitov, A.V. Chubukov, Nat. Phys. **8**, 158 (2012)
26. W. Wu, M.M. Scherer, C. Honerkamp, K. Le Hur, Phys. Rev. B **87**, 094521 (2013)
27. R. Nandkishore, L.S. Levitov, A.V. Chubukov, Nat. Phys. **8**, 158 (2011)
28. J.L. McChesney, A. Bostwick, T. Ohta, T. Seyller, K. Horn, J. González, E. Rotenberg, Phys. Rev. Lett. **104**, 136803 (2010)
29. A.M. Black-Schaffer, S. Doniach, Phys. Rev. B **75**, 134512 (2007)
30. S. Zhang, M. Tanaka, T. Onimaru, T. Takabatake, Y. Isikawa, S. Yamanaka, Supercond. Sci. Technol. **26**, 045017 (2013)
31. A. Ii, A. Yamakage, K. Yada, M. Sato, Y. Tanaka, Phys. Rev. B **86**, 174512 (2012)
32. N. Kopnin, *Vortices in Type-II Superconductors: Structure and Dynamics* (Oxford University Press, Oxford, 2001)
33. B. Rosenstein, D.P. Li, Rev. Mod. Phys. **82**, 109 (2010)
34. C. Caroli, P.G. de Gennes, J. Matricon, Phys. Lett. **9**, 307 (1964)
35. P.G. DeGennes, *Superconductivity of Metals and Alloys* (W.A. Benjamin, New York, 1966)
36. J.D. Shore, M. Huang, A.T. Dorsey, J.P. Sethna, Phys. Rev. Lett. **62**, 3089 (1989)
37. F. Gygi, M. Schlüter, Phys. Rev. B **41**, 822 (1990)
38. F. Gygi, M. Schlüter, Phys. Rev. B **43**, 7609 (1991)
39. C. Berthod, Phys. Rev. B **71**, 134513 (2005)
40. B. Janko, J.D. Shore, Phys. Rev. B **46**, 9270 (1992)

41. G.E. Volovik, JETP Lett. **70**, 609 (1999)
42. F. Wilczek, Nat. Phys. **5**, 619 (2009)
43. A.S. Mel'nikov, A.V. Samokhvalov, M.N. Zubarev, Phys. Rev. B **79**, 134529 (2009)
44. B. Rosenstein, I. Shapiro, E. Deutch, B.Y. Shapiro, Phys. Rev. B **84**, 134521 (2011)
45. B. Rosenstein, I. Shapiro, B.Ya. Shapiro, J. Phys. Condens. Matter **25**, 075701 (2013)
46. N. Kopnin, Phys. Rev. B **57**, 11775 (1998)
47. M. Kato, K. Maki, Europhys. Lett. **54**, 800 (2001)
48. Y. Morita, M. Kohmoto, K. Maki, Europhys. Lett. **40**, 207 (1997)
49. M. Kato, K. Maki, Prog. Theor. Phys. **107**, 941 (2002)
50. H.F. Hess, R.B. Robinson, R.C. Dynes, J.M. Valles, J.V. Waszczak, Phys. Rev. Lett. **62**, 214 (1989)
51. I. Maggio-Aprile, Ch. Renner, A. Erb, E. Walker, Ø. Fischer, Phys. Rev. Lett. **75**, 2754 (1995)
52. L. Shan, Y.-L. Wang, B. Shen, B. Zeng, Y. Huang, A. Li, D. Wang, H. Yang, C. Ren, Q.-H. Wang, S.H. Pan, H.-H. Wen, Nat. Phys. **7**, 325 (2011)
53. Y. Morjita, M. Kohmoto, K. Maki, Int. J. Mod. Phys. B **12**, 989 (1998)
54. J.B. Ketterson, S.N. Song, Superconductivity. Northweat University (1999)
55. J.X. Zhu, Physica C **340**, 230 (2000)
56. S.H. Simon, P.A. Lee, Phys. Rev. Lett. **78**, 1548 (1997)
57. M.E. Zhitomirsky, V.-H. Dao, Phys. Rev. B **69**, 054508 (2004)
58. G. Catelani, E.A. Yuzbashyan, Phys. Rev. A **81**, 033629 (2010)
59. N.B. Kopnin, A.S. Mel'nikov, V.M. Vinokur, Phys. Rev. B **68**, 054528 (2003)
60. N.B. Kopnin, A.S. Mel'nikov, V.I. Pozdnyakova, D.A. Ryzhov, I.A. Shereshevskii, V.M. Vinokur, Phys. Rev. B **75**, 024514 (2007)
61. K. Steinberg, M. Scheffler, M. Dressel, Phys. Rev. B **77**, 214517 (2008)
62. J.H. Davies, *The Physics of Low-Dimensional Semiconductors* (Cambridge University Press, New York, 1998)